MCP Papers in Press. Published on March 5, 2018 as Manuscript RA117.000069

Proteomics of *Aspergillus fumigatus* conidia-containing phagolysosomes identifies processes governing immune evasion

Hella Schmidt[1], Sebastian Vlaic[2], Thomas Krüger[1], Franziska Schmidt[1], Johannes Balkenhol[3], Thomas Dandekar[3], Reinhard Guthke[2], Olaf Kniemeyer[1], Thorsten Heinekamp[1], Axel A. Brakhage[1, 4,*]

[1] Department of Molecular and Applied Microbiology, Leibniz Institute for Natural Product Research and Infection Biology – Hans Knöll Institute (HKI), Jena, Germany

[2] Systems Biology and Bioinformatics, Leibniz Institute for Natural Product Research and Infection Biology (HKI), Jena, Germany

[3] Department of Bioinformatics, Julius Maximilians University Würzburg, Würzburg, Germany

[4] Department of Microbiology and Molecular Biology, Institute of Microbiology, Friedrich Schiller University, Jena, Germany

Hella Schmidt, hella.schmidt@leibniz-hki.de; Sebastian Vlaic, sebastian.vlaic@leibniz-hki.de; Thomas Krüger, thomas.krueger@leibniz-hki.de; Franziska Schmidt, franziska.schmidt@leibniz-hki.de; Johannes Balkenhohl, johannes.balkenhol@uni-wuerzburg.de; Thomas Dandekar, dandekar@biozentrum.uni-wuerzburg.de; Reinhard Guthke, reinhard.guthke@leibniz-hki.de; Olaf Kniemeyer, olaf.kniemeyer@leibniz-hki.de; Thorsten Heinekamp, thorsten.heinekamp@leibniz-hki.de

* Corresponding author:
Axel A. Brakhage
Department of Molecular and Applied Microbiology
Leibniz Institute for Natural Product Research and Infection Biology (HKI)
Adolf Reichwein Str. 23, 07745 Jena, Germany
Phone: +49 – (0)3641 532 1000
Fax: +49 – (0)3641 532 0802
Email: axel.brakhage@leibniz-hki.de

Running Title: Proteomics of conidia-containing phagolysosomes

Abbreviations

1,8-DHN	1,8-dihydroxynaphthalene
A. fumigatus	*Aspergillus fumigatus*
AGC	automatic gain control
AMM	*Aspergillus* minimal medium
Atg	autophagy-related genes
C. albicans	*Candida albicans*
C. neoformans	*Cryptococcus neoformans*
CD	cluster of differentiation
CFW	calcofluor white
CoA	coenzyme A
CSFR	colony-stimulating factor receptor
DMEM	Dulbecco's modified eagle medium
EEA	early endosomal antigen
ERK	extracellular signal-regulated kinase
FBS	fetal bovine serum
FcR	fragment crystallizable receptor
FDR	false discovery rate
FWHM	full width of half maximum
GAP	GTPase-activating protein
GAPDH	glyceraldehyde-3-phosphate dehydrogenase
GEF	guanine nucleotide exchange factor
GO	gene ontology
HCD	higher-energy collisional dissociation
HPI	host-pathogen interaction
HRP	horse-reddish peroxidase
Hsp	heat shock protein
IgG	immunoglobulin G
KEGG	Kyoto encyclopedia of genes and genomes
Lamp	lysosome-associated membrane protein
LAP	LC3-associated phagocytosis
LC3	microtubule-associated protein 1 light chain 3

LSM	laser scanning microscope
MAPK	mitogen-activated protein kinase
MOI	multiplicity of infection
mRNA	messenger ribonucleic acid
mTOR	molecular target of rapamycin
Nduf	NADH dehydrogenase
NOX	NADPH oxidase
OXPHOS	oxidative phosphorylation
P. brasiliensis	*Paracoccidioides brasiliensis*
PD	Proteome Discoverer
PE	phosphatidylethanolamine
PI3K	phosphoinositide-3-kinase
pks	polyketide synthase
PMN	polymorphonuclear
PPI	protein-protein interaction
PSM	peptide spectrum matches
ROS	reactive oxygen species
Rubicon	Run domain beclin-1-interacting and cysteine-rich domain-containing protein
SNAP	synaptosomal-associated protein
SNARE	soluble N-ethylmaleimide-sensitive-factor attachment receptor
TCEP	tris-(2-carboxyethyl)-phosphine
TEAB	tetraethylammonium bicarbonate
Tef	translation elongation factor
TLR	toll-like receptor
Vamp	vesicle-associated membrane protein
vATPase	vacuolar ATPase
Vcam	vascular cell adhesion molecule
Vti	vesicle transport through interaction with t-SNAREs
wt	wild type

Summary

Invasive infections by the human pathogenic fungus *Aspergillus fumigatus* start with the outgrowth of asexual, airborne spores (conidia) into the lung tissue of immunocompromised patients. The resident alveolar macrophages phagocytose conidia, which end up in phagolysosomes. However, *A. fumigatus* conidia resist phagocytic degradation to a certain degree. This is mainly attributable to the pigment 1,8-dihydroxynaphthalene (DHN) melanin located in the cell wall of conidia, which manipulates the phagolysosomal maturation and prevents their intracellular killing. To get insight in the underlying molecular mechanisms, we comparatively analyzed proteins of mouse macrophage phagolysosomes containing melanized wild-type (wt) or non-melanized *pksP* mutant conidia. For this purpose, a protocol to isolate conidia-containing phagolysosomes was established and a reference protein map of phagolysosomes was generated. We identified 637 host and 22 *A. fumigatus* proteins that were differentially abundant in the phagolysosome. 472 of the host proteins were overrepresented in the *pksP* mutant and 165 in the wt conidia-containing phagolysosome. Eight of the fungal proteins were produced only in *pksP* mutant and 14 proteins in wt conidia-containing phagolysosomes. Bioinformatical analysis compiled a regulatory module, which indicates host processes affected by the fungus. These processes include vATPase-driven phagolysosomal acidification, Rab5 and Vamp8-dependent endocytic trafficking, signaling pathways, as well as recruitment of the Lamp1 phagolysosomal maturation marker and the lysosomal cysteine protease cathepsin Z. Western blot and immunofluorescence analyses confirmed the proteome data and moreover showed differential abundance of the major metabolic regulator mTOR. Taken together, with the help of a protocol optimized to isolate *A. fumigatus* conidia-containing phagolysosomes and a potent bioinformatics algorithm, we were able to confirm *A. fumigatus* conidia-dependent modification of phagolysosomal processes that have been described before and beyond that, identify pathways that have not been implicated in *A. fumigatus* evasion strategy, yet.

Mass spectrometry proteomics data are available *via* ProteomeXchange with identifiers PXD005724 and PXD006134.

Introduction

Infections with the opportunistic pathogen *Aspergillus fumigatus* pose a major threat to human health. It is estimated that there are worldwide more than 200,000 cases of invasive aspergillosis per year affecting patients with a severe underlying immune suppression due to hematologic diseases, genetic immune deficiencies or solid organ or hematopoietic stem cell transplantation (1, 2). *A. fumigatus* produces asexual spores (conidia) that are distributed *via* the air. Upon inhalation conidia reach the lower airway tract of human individuals. In immunocompromised hosts, the impaired immune cell function allows fungal colonization of the lung tissue and the establishment of a life-threatening infection (3).

Resident alveolar macrophages belong to the first line of immune defense (4). They are activated by fungal surface structures such as the β-1,3-glucans of the conidial cell wall which bind to the C-type lectin receptor Dectin-1 and thereby inducing phagocytosis. Activated macrophages engulf conidia in a phagosome, which gradually acquires biocidal properties from fusion with lysosomes to generate a mature phagolysosome with acidic luminal pH due to vacuolar ATPase (vATPase) activity (4, 5). Small Rab GTPases govern the dynamic fusion and fission processes required for generation of mature phagolysosomes and thus belong to the targets of intracellular pathogens to interfere with the maturation process (6-8). For example, *Mycobacterium tuberculosis* prevents the recruitment of Rab14 to the phagolysosome and thereby arrests its maturation (7).

The grey-green pigment of *A. fumigatus* conidia consists of 1,8-dihydroxynaphthalene (DHN) melanin that represents an important virulence determinant (9). Due to melanin wt conidia are able to reduce the production of and quench reactive oxygen species (ROS) and thus lower the amounts of ROS in the phagolysosome. Furthermore, wt conidia inhibit apoptosis, survive in host cells, germinate and cause damage to host cells (10-13). A mutant strain producing white conidia was shown to be defective in the polyketide synthase gene *pksP* and, hence, unable to produce DHN melanin (12). Inside the phagolysosome *pksP* conidia are faster degraded than wt conidia by luminal acidification and activity of lytic enzymes (14). DHN melanin is the crucial and sufficient factor to block acidification as demonstrated in experiments with melanin particles, *i.e.*, 'melanin ghosts' (14). However, the molecular mechanisms of the interference of the wt conidium with the phagosomal maturation are still not well understood. Previous work of our group showed that *A. fumigatus* wt conidia-containing phagolysosomes fused with vesicles of the endocytic compartment to a certain extent, but showed reduced acidification required to establish the fungicidal environment for degradation of conidia (13).

The activity of the vATPase is essential to drive the acidification of conidia-containing phagolysosomes (14).

For several pathogenic microorganisms, proteomic studies unraveled the specific protein composition of phagolysosomes for a better understanding of the phagosomal maturation process and its modulation by pathogens (15-23). These studies demonstrated that the protein composition of the phagosome is highly dynamic, specific for the ingested particle, depends on the stage of phagosomal maturation, the type or cell line and the activation status of the phagocyte. Therefore, we set out to analyze the phagolysosomal proteome after phagocytosis of wt and *pksP* mutant conidia in order to shed light on processes inhibited by wt conidia during the maturation of phagosomes. In this study, a magnetic label–based purification protocol for conidia-containing phagolysosomes and the application of a label-free protein quantification method was developed. Bioinformatics was employed to determine the regulatory modules of differentially abundant proteins of the macrophage phagolysosome. We confirmed a differential regulation of vATPase subunits and apoptosis induction. These processes were already identified by us in previous studies as targets of *A. fumigatus* for immune evasion. Moreover, the combination of quantitative proteomics and bioinformatics led to the identification of *A. fumigatus*-modulated processes and of macrophage intracellular functions. These processes include vesicle trafficking and endocytosis, degradative and immune functions of the phagolysosome, NADPH oxidase activity to produce ROS, MAPK and mTOR signaling as well as metabolic reprogramming of the macrophage.

Experimental procedures

Materials and chemicals

Primary antibodies were purchased from Abcam (Ndufb9 ab200198; Vamp8 ab76021), Santa Cruz Biotechnology (Lamp1 sc-19992, Cathepsin D sc-10725), Cell Signaling Technologies (mTOR #2983; Rab5 #3547) and Thermo Fisher Scientific (Cathepsin Z PA5-47048; Rab7A PA5-22959). Secondary antibodies for western blot analyses were goat anti-rabbit IgG-HRP (sc-2030), goat anti-rat IgG-HRP (sc-2031) from Santa Cruz Biotechnology and rabbit anti-goat IgG-HRP (#31402) from Thermo Fisher Scientific. Secondary antibody for immunofluorescence was goat anti-rabbit IgG-DyLight 633 (#35562, Thermo Fisher Scientific).

Cells and A. fumigatus strains

Mouse RAW 264.7 macrophages (ATCC TIB-71) were cultured in DMEM (Biozyme, Germany) with FBS (GE Healthcare, Germany), ultraglutamine (Biozyme) and gentamycin at 37 °C with 5 % (v/v) CO_2. *A. fumigatus* wt strain ATCC 46645 and *pksP* mutant (11, 12) strain were cultured on *Aspergillus* minimal medium (AMM) agar plates. After 5 days of incubation at 37 °C, conidia were harvested in 10 ml of 0.9 % (w/v) NaCl / 0.01 % (v/v) Tween 80 (Roth, Germany) using a cell scraper and filtered through a 40 µm cell strainer (BD, Germany) to remove mycelia. The number of conidia was counted using a hemocytometer.

Magnetic labeling of conidia and purification of phagolysosomes

The protocol for isolation of conidia-containing phagolysosomes by magnetic separation was adapted from Steinhäuser *et al.* (24). 2×10^8 wt conidia were labeled with 10 mg/mL EZ link sulfo-NHS-LC biotin (Thermo Fisher Scientific) in 50 mM Na_2CO_3. Initial experiments demonstrated that for the same amount of *pksP* mutant conidia 10 µg/mL NHS-biotin linker yielded a comparable efficiency of magnetic loading. Cells were incubated with the linker for 2 h at 4 °C on a rotator and then washed. 50 µL of the streptavidin-coupled magnetic beads (Miltenyi, Germany) in the concentration provided by the supplier (Thermo Fisher Scientific) were added in labeling buffer (PBS with 2 mM EDTA) to the conidia suspension and incubated for 15 min at 4 °C on a rotator. Co-incubation was performed in 4-well plates. Each well contained 4×10^6 RAW 264.7 macrophage cells.

For infection, an MOI of 5 was used, which corresponds to $2x10^7$ magnetically-labeled conidia. An MOI of 5 yielded the required amount of protein needed for the analysis of the subcellular proteome. Co-incubation was stopped after 2 h. The cells were washed with PBS, scratched off and collected in homogenization buffer (3 mM imidazole, 250 mM sucrose, pH 7.4 and proteinase inhibitors (c*O*mplete, Roche, Switzerland) and benzonase nuclease (Merck Millipore, Germany)). Cell lysis was achieved by pressing the cell suspension 60 times through a needle (27G) and was monitored microscopically. DNase (Epicentre, USA) was added and the lysate was incubated for 5 min at 37 °C. For sampling of the whole cell proteome, proteins of the lysate were precipitated and processed as described below. To purify the phagolysosomal fraction the lysate was loaded onto a QuadroMACS separator (Miltenyi). Phagolysosomes with magnetically labeled conidia were retained on the stand by magnetic force and proteins were directly eluted from the column with 98 °C heated elution buffer (2 % (w/v) SDS, 100 mM TEAB, 10 % (v/v) glycerol, 1 mM TCEP).

Processing of proteins

The eluted protein solution was reduced by evaporation in a SpeedVac at 60 °C to a volume of 100 µL. Proteins were precipitated with methanol and chloroform as described elsewhere (25) and protein concentrations determined using the Direct Detect Infrared Spectrometer (Merck Millipore). 100 µg of the precipitated protein was resuspended in 100 mM TEAB buffer, proteins were reduced with 200 mM TCEP, alkylated with 375 mM iodoacetamide and digested with 4 µg trypsin (SERVA) over night at 37 °C. The reaction was stopped with formic acid and the sample was resuspended in acetonitrile, TFA for LC-MS/MS analysis.

Western blot

16 and 8 µg of protein were loaded on a 4-12 % (w/v) Bis-Tris Protein Gel (NuPAGE, Thermo Fisher Scientific) and separated by SDS-PAGE in 1x MES running buffer (Thermo Fisher Scientific). The protein was blotted with a semi-dry blot device (Bio-Rad, Germany) onto a low fluorescent PVDF membrane (GE Healthcare Life Sciences) using a Tris/glycine transfer buffer (25 mM Tris-HCl, 192 mM glycine, 20 % (v/v) methanol). The blot was incubated with specific primary antibodies as specified and horse reddish peroxidase-coupled secondary antibodies were used for detection. The reaction mix of the Smart Protein Layer Kit (NH DyeAGNOSTICS, Germany) was added to the sample prior to the experiment for a fluorescent labeling of the total amount of proteins, which was used as a loading control (26). Fluorescence and chemiluminescence were detected with the Fusion FX7 system (Vilber Lourmat,

Germany) and signal intensities and quantifications were determined with the Bio-1D analysis software (Vilber Lourmat) as described in the manufacturer's instructions. Western blots were conducted for each of the three replicates of conidia-containing phagolysosome purifications.

Experimental design and statistical rational

By using a quantitative label-free proteomics approach, we compared the subproteome of enriched phagolysosomes containing melanized wt with non-melanized pksP mutant conidia. Three biological replicates of wild-type and *pksP* conidia-containing phagolysosomes were measured each in three analytical replicates. Analytical replicates were treated as fractions (merged together for database searches) while biological replicates were analyzed independently of each other. Mean values and standard deviations for biological replicates of each comparison group were calculated. Differentially abundant proteins were determined using a $\log_2$ fold-change cut-off threshold of 1. By the identification of regulatory modules an additional level of information was provided. A regulatory module denotes a region in the organism-specific protein-protein interaction network, which is significantly enriched with differentially abundant proteins. Proteins that are differentially abundant but not within the module are disregarded since they are not well connected with other differentially abundant proteins. Thus, confidence in the reliability of the measured fold-change is gained by additional topological information from the protein-protein interaction network. For evaluation of the enrichment of the phagolysosomal fraction, we further compared the phagolysosome-enriched subcellular proteome with the whole cell proteome of macrophages, which had ingested either wt or *pksP* conidia of *A. fumigatus*. The whole cell sample was generated once and analyzed in three technical replicates.

LC-MS/MS analysis of protein samples

Two different methods were applied. For the sub-proteome analysis of the conidia-containing phagolysosomal fraction an analytical method designated as method M#1 was used. For comparison of the phagolysosomal sub-proteome with the whole cell proteome method M#2 was applied.

LC-MS/MS analysis was carried out on an Ultimate 3000 RSLC nano system coupled to a QExactive Plus mass spectrometer (both Thermo Fisher Scientific). Peptides were enriched on a nano-trap column (Acclaim PepMap 100, length 20 mm, diameter 75 µm, particle size 3 µm) at a flow rate of 5 µL/min. Trapped peptides were separated after a valve switch on Acclaim PepMap RSLC nano columns with 150

mm (M#1) or 500 mm (M#2) length (Thermo Fisher Scientific). The mobile phase consisted of eluent A) 0.1% (v/v) formic acid in H_2O and eluent B) 0.1% (v/v) formic acid in 90/10 ACN/H_2O. We applied either 135 min (M#1) or 360 min (M#2) gradient elution using the following gradients:

M#1: 0-5 min at 4% B, 10 min at 6.5% B, 15 min at 7.5% B, 20 min at 8% B, 25 min at 8.6% B, 30 min at 9.2% B, 35 min at 9.9% B, 40 min at 10.6% B, 45 min at 11.3% B, 50 min at 12.2% B, 55 min at 13.4% B, 60 min at 14.9% B, 65 min at 17% B, 70 min at 19.1% B, 75 min at 22.4% B, 80 min at 26% B, 88 min at 32% B, 94 min at 40% B, 100 min at 52% B, 103 min at 68% B, 106-114 min at 96% B, 115-135 min at 4% B.

M#2: 0-4 min at 4% B, 90 min at 9% B, 130 min at 12.5% B, 180 min at 17% B, 200 min at 20% B, 220 min at 24% B, 250 min at 35% B, 260 min at 44% B, 265 min at 50% B, 270 min at 55% B, 275 min at 70% B, 280-290 min at 96% B, 291-360 min at 4% B.

Positively charged ions were generated with a stainless steel emitter at 2.2 kV spray voltage using a Nanospray Flex Ion Source (Thermo Fisher Scientific). The MS instrument was operated in Full MS / dd MS^2 (TopN) mode. Precursor ions were measured in full scan mode within a mass range of either m/z 300-1600 (M#1) or m/z 300-1500 (M#2) at a resolution of 70k/140k FWHM (M#1/M#2) using a maximum injection time of 120 ms and an AGC (automatic gain control) target of 10^6. Up to 10 of the most abundant precursor ions per scan cycle with an assigned charge state of z = 2-6 were selected for data-dependent acquisition using an isolation width of m/z 2.0. HCD fragmentation was conducted at a normalized collision energy of 30 V using N_2. Dynamic exclusion of precursor ions was 35 s (M#1) or 40 s (M#2). Fragment ions were monitored at a resolution of 17.5k (FWHM) using a maximum injection time of 120 ms and an AGC target of $2x10^5$. The fixed first mass was set to m/z 120. The LC-MS/MS instrument was operated by means of the Thermo/Dionex Chromeleon Xpress 6.8 software and the Thermo QExactive Plus Tune / Xcalibur 3.0.63 software.

Protein database search and label-free quantitation

Thermo raw files were processed by the Proteome Discoverer (PD) software v1.4 (M#1) and v2.1 (M#2) (Thermo Fisher Scientific). Tandem mass spectra were searched against databases (download date 21/09/2016) of *Mus musculus* (UniProt) and *A. fumigatus* (*Aspergillus* Genome Database, AspGD). It was searched against 66,868 database entries (protein sequences) using the algorithms of Mascot v2.4.1 (Matrix Science, UK), Sequest HT (as integral part of the Thermo software suite Proteome Discoverer 1.4.0.288 (M#1) and 2.1.0.81 (M#2)) and MS Amanda (release version 1.0.0.4756). Two missed

cleavages were allowed for tryptic peptides. The precursor mass tolerance was 10 ppm and the fragment mass tolerance was 0.02 Da. Dynamic modification was oxidation of methionine. Static modification was cysteine carbamidomethylation. Percolator node and a reverse decoy database was used for *q*-value validation of the peptide spectral matches (PSMs) using a strict target false discovery (FDR) rate of < 1%. At least 2 peptides per protein were required for positive protein hits. Label-free quantification was performed with the precursor ions area - Top3 method included in PD. It compares the 3 most abundant peptides of each protein by using the peak area of the respective precursor ion (27). The mass tolerance was set to 2 ppm and the signal-to-noise ratio should be > 3. The abundance values were normalized based on the total peptide amount. Only unique peptides were considered for quantification. The significance threshold for differential protein regulation was set to factor ≥ 2.0 (up- or down-regulation). The mass spectrometry proteomics data were deposited at the ProteomeXchange Consortium *via* the PRIDE (28) partner repository with the dataset identifiers PXD005724, 10.6019/PXD005724.

Identification of the regulatory module from LC-MS/MS data

Identification of the murine regulatory module was performed using ModuleDiscoverer (29) similar to the approach described in (30). In brief, differentially abundant proteins were mapped onto the murine protein-protein interaction network obtained from the STRING database. Identification of the regulatory module was then performed by the extraction of network regions that are significantly enriched with differentially abundant proteins. These sub-networks were analyzed regarding their biological function using the GOstats package for R (31). Mapping of different protein identifiers was achieved by applying the org.Mm.eg.db annotation package for R (32) as well as the Ensembl BioMarts resource (33) using the biomaRt package for R (34). A detailed description is provided in the supplement.

Prediction of host-pathogen interactions

In order to predict the protein interactions of the *M. musculus* macrophages and *A. fumigatus* conidia within the phagolysosome, the regulatory module and the detected fungal proteins were mapped to an existing database of predicted host-pathogen interactions (HPI). The dataset HPI was calculated by using experimental verified interactions from model organisms. These sources for interactions deliver the backbone to predict interfacial interaction of host and pathogen (35). By using traits that characterize the source interacting proteins, such as amino acid sequence, GO annotation, pathway membership, expression level, or domain information, pairs of interacting proteins of host and pathogen could be set

up, filtered and refined. The establishment of protein pairs, as well as the filtering was exhibited similar to Remmele *et al*. (35), whereas the refinement steps involved a scoring system based on experimental exchange of orthologs and analog prediction methods. Details about the prediction and scoring method are given in the supplementary information.

Immunofluorescence

Conidia were stained with 0.1 mg/mL calcofluor white (CFW, Fluorescence Brightener 26, Sigma Aldrich, Germany) for 25 min at room temperature or with 0.1 mg/mL fluorescein isothiocyanate (FITC, Sigma-Aldrich) in 100 mM Na_2CO_3 for 30 min at 37 °C. Cells were infected with conidia at an MOI of 2 and co-incubated for 2 h at 37 °C with 5 % (v/v) CO_2. After co-incubation, cells were fixed with 3.7 % (v/v) formaldehyde for 10 min at room temperature. For immunofluorescence detection, cells were treated with 0.25 % (v/v) Triton X-100 (VWR, Germany), blocked with 3 % (w/v) bovine serum albumin (Sigma-Aldrich) and 3 % (v/v) goat serum (Santa Cruz Biotechnology) and then incubated overnight at 4 °C with the primary antibody. Secondary antibody was added for 1 h at room temperature. All images were acquired on a Zeiss LSM 780 confocal microscope with a Zeiss Plan-appochromat 63×/1.4 oil objective. Three technical and two biological replicates were analyzed for each strain. Six images were taken per technical replicate, which resulted in 36 images in total per strain. The total number of ingested conidia per image was determined. The conidia-containing phagolysosomes with a specific fluorescence from the target molecule, as indicated by a circular fluorescence signal around the conidium, were considered positive for the desired marker. With the number of positive phagolysosomes and the total number of ingested conidia the ratio of target-positive phagolysosomes was determined.

RESULTS

Development of a protocol for isolation of conidia-containing phagolysosomes

To address the question, whether the manipulation of the phagosome maturation by wt conidia is reflected in the phagolysosomal proteome, proteins were extracted from phagolysosomes containing melanized wt and non-melanized *pksP* mutant conidia based on a protocol for the isolation of *Mycobacteria*-containing phagolysosomes (24). Magnetic labeling of conidia enabled the isolation of the phagolysosomal fraction after lysis of infected macrophages (Fig. 1). The concentration of NHS-biotin linker was adjusted to the different surface properties (11) of the two types of conidia. Therefore, linker-binding capacities of conidia of the two strains were monitored microscopically by the addition of streptavidin-coupled Alexa-fluorophore (data not shown). Magnetic beads were bound to the conidia by a streptavidin tag. To exclude effects of labeling on phagocytosis and intracellular processing of the conidia, phagocytosis ratio and the ratio of acidified phagolysosomes of labeled and unlabeled wt and *pksP* mutant conidia were determined. After 2 hours of co-incubation of conidia with macrophages, no differences in phagocytosis of labeled and unlabeled conidia were detected (Fig. 2A). Furthermore, 16.8% and 20.8% of labeled and unlabeled wt conidia-containing phagolysosomes, respectively, and 68.4 % and 77.1 % of labeled and unlabeled *pksP* mutant conidia-containing phagolysosomes, respectively, were acidified (Fig. 2B). Thus, the label on the conidial surface had no significant effect on the acidification of the phagolysosome.

Wt and *pksP* conidia-containing phagolysosomes were isolated two hours after infection of RAW 264.7 macrophages, because at this time point acidified phagolysosomes had been formed (36). After co-incubation of conidia and macrophages, shearing of cells provided the best method to ensure a thorough cell lysis without affecting the integrity of the phagolysosomes. To determine the integrity and quality of the isolated phagolysosomes, membranes were stained with the lipophilic dye DiD. The localization of fluorescent microbeads (3000 MW Dextran beads, Thermo Fisher Scientific), which are taken up by pinocytosis and transferred *via* lysosomes to the phagolysosome, was monitored microscopically. A clear fluorescence signal of DiD and dextran beads surrounded the conidia indicating the presence of a continuous and intact phagolysosomal membrane (Fig. 2C). The complete lysate was loaded onto a magnetic column and washed extensively to remove contaminating cell debris. The proteins of retained phagolysosomes were extracted on the column, and the flow-through was collected, concentrated and processed for LC-MS/MS measurements (Fig. 1).

Identification of differentially abundant proteins from LC-MS/MS data

LC-MS/MS measurement and protein identification resulted in a dual proteome set consisting of 2431 murine phagolysosomal and 65 *A. fumigatus* proteins (Table S1). 95 % of the proteins were detected in both wt und *pksP* mutant conidia-containing phagolysosomes, suggesting that quantitative differences predominate. To identify the differences, a label-free quantification was performed using the 'Top Three' method (27) and the relative abundance of proteins in *pksP* mutant *versus* wt conidia-containing phagolysosomes was calculated. Based on a $\log_2$ fold-change cut-off threshold of 1, we identified 637 differentially abundant proteins in the phagolysosome and 22 differentially abundant proteins from *A. fumigatus.* Of the 637 regulated proteins of the phagolysosome, 472 were overrepresented in the *pksP* mutant conidia-containing phagolysosome and 165 in the wt conidia-containing phagolysosome. On the fungal side, 8 proteins were found to be specific for *pksP* mutant conidia and 14 proteins for wt conidia.

For a quality control of the purification protocol the phagolysosomal proteome was compared to the whole cell proteome, which was obtained by extraction of proteins directly from the lysate of macrophages infected with wt or *pksP* mutant conidia. The whole cell proteome comprised 1986 murine proteins (Table S2). 53 % of total phagolysosomal proteins and 39 % of differentially abundant proteins in the phagolysosome were also detected in the whole cell proteome. Thus, a proportion of 47 % of total phagolysosomal proteins and 61 % of differentially produced proteins was only found in the purified sample, indicating, that the purification protocol of phagolysosomes allowed for enrichment of these organelles. This assumption was further substantiated because proteins assigned to the gene ontology (GO) 'lysosome' (count = 69, *p*-value = $5.3\text{x}10^{-6}$) and 'lysosomal membrane' (count = 63, *p*-value = $3{,}2\text{x}10^{-10}$) showed a strong enrichment in the phagolysosomal fraction compared to the whole cell proteome (count = 41, *p*-value 0.06 and count = 40, *p*-value = $1.8\text{x}10^{-4}$). Further, the *p*-value for the GO-term 'cytosol' is larger in the phagolysosomal fraction ($8.5\text{x}10^{-21}$, count = 362) compared to the *p*-value in the whole cell sample (*p*-value = $4.2\text{x}10^{-41}$, count = 359) indicating that the phagolysosomal fraction contains less signal from the cytosol compared to the whole cell samples. Based on this evaluation, the purification protocol clearly accomplished a concentration of the phagolysosomal fraction.

Regulatory module implies interaction of regulated proteins

To deduce regulated processes from the dataset of differentially abundant proteins, we used a bioinformatics approach that identified regulatory modules within the protein-protein interaction (PPI) network provided by the STRING database (37). This analysis was based on the projection of

experimentally identified differentially abundant proteins. As a result, a host regulatory module was defined that contained the regulated proteins but also non-regulated and non-detected proteins depicted as knots and their connections visualized as edges. Within the network, submodules represent groups of proteins with a higher connectivity based on STRING that are functionally or structurally related.

The assembled host regulatory module is composed of 302 proteins connected by 3448 edges. 178 of the 302 proteins were detected by LC-MS/MS. 109 of these 178 proteins were identified as differentially abundant. 79 proteins were enriched in the *pksP* mutant and 30 in the wt conidia-containing phagolysosome. In the host regulatory module 17 submodules were classified. 14 of these submodules comprising five or more proteins were considered for further discussion and used in enrichment analysis of GO and KEGG pathway terms (Table S3). The submodules representing vATPase-dependent vacuolar acidification, signaling, endocytosis and vesicle transport, immune response, generation of ROS *via* NADPH oxidase and electron transport chain were the focus for further validation experiments and discussion (Fig. 3). In detail, these submodules include proteins with annotated functions in MAPK signaling pathway, actin polymerization, SNARE-mediated membrane trafficking and Rab GTPase-regulated vesicle fusion, hydrolytic activities and NADPH oxidase-dependent ROS production.

To verify the data obtained by LC-MS/MS analysis, label-free quantification and the regulatory module analysis, the abundances of several representative proteins were quantified by western blot analyses or immunofluorescence (Fig. 4). First, to exclude that magnetic labeling interferes with recruitment of phagolysosomal proteins the localization of cathepsin D was monitored by immunofluorescence. Both, labeled and unlabeled wt conidia reduced recruitment of cathepsin D to the phagolysosomal membrane, whereas *pksP* conidia-containing phagolysosomes showed a typical pattern of cathepsin D recruitment, independent of magnetic labeling (Fig. 4A). Representative proteins included proteins enriched in *pksP* conidia-containing phagolysosomes: Cathepsin Z, a lysosomal protease, which was 2-fold higher abundant; Lamp1, a phagolysosomal marker protein represented in the 'endocytosis' module with a 3.8-fold higher abundance; Nduf9, a component of the NADH dehydrogenase complex represented in the module 'electron transport chain' with 5.9-fold higher abundance. The higher abundance of selected proteins in *pksP* conidia-containing phagolysosomes was confirmed by western blot analysis (Fig. 4B). Because we found LAMTOR, a regulator of the mTOR signaling pathway, enriched in *pksP* conidia-containing phagolysosomes, and, secondly, the regulatory module indicated a regulation of carboxylic acid metabolism and cellular respiration, we analyzed the abundance of the kinase mTOR.

Both aforementioned processes are potentially controlled by mTOR. Although not detected by LC-MS/MS, we could confirm a differential regulation of mTOR in conidia-containing phagolysosomes by western blot (Fig. 4B). The vesicle trafficking protein 8 (Vamp8), which was assigned to the 'vesicle trafficking' module and which was 2.8-fold enriched in *pksP* conidia-containing phagolysosomes, was analyzed for its localization by immunofluorescence. A differential recruitment was clearly confirmed (Fig. 4C).

Fungal proteins in the phagolysosome

The host regulatory module provided information about processes that are regulated in the macrophage upon phagocytosis of *A. fumigatus* conidia. The dual proteome analysis allowed us to investigate differentially abundant fungal proteins as potential effectors interfering with the host endocytic pathway. It is likely that fungal proteins in the phagolysosome are either actively secreted or released from the fungal cell surface. However, it needs to be considered that the two strains face different conditions: While *pksP* mutant conidia are exposed to an acidic environment and tackled by phagolysosomal degrading enzymes 2 h after phagocytosis, the wt conidia reside in more favorable conditions in a phagolysosome with neutral pH. Accordingly, the fungal proteome enriched from *pksP* mutant conidia-containing phagolysosomes was composed of proteins induced upon oxidative stress or upon encounter with immune cells, *e.g.*, a GTPase regulating vesicular transport, an RNA helicase, alcohol dehydrogenases and a transaldolase of the pentose phosphate pathway (Table S4).

Proteins enriched in wt conidia-containing phagolysosomes included a catalase, drug response and mitochondrial unfolded protein response elements and glyceraldehyde-3-phosphate dehydrogenase (GAPDH). Further proteins were histone H2A1, a component of ribosome biogenesis, transcription and mRNA processing, the signaling protein 14-3-3 and a high abundant conidial protein with unknown function that was found by Asif *et al.* (38) to be present on conidia (Table S5).

DISCUSSION

Here, we set out to characterize the phagolysosomal proteome and to identify phagolysosomal proteins and processes that are altered after phagocytosis of melanized *A. fumigatus* conidia to allow their survival inside the macrophage. The phagolysosome is the place of the direct interaction between conidia and the host, hence, it can be expected that modifications in its protein composition influence its fungicidal activity. On the level of the whole cell, changes in abundance of proteins in specific organelles like the phagolysosome might be masked *e.g*. by highly abundant cytosolic proteins. Therefore, we analyzed the proteomes of both whole macrophage cells and phagolysosomes. Because previously we showed that DHN melanin of the conidia interferes with the maturation of phagolysosomes (14) we compared the phagolysosomal proteomes of macrophages, which were infected either with wt or non-pigmented *pksP* mutant conidia of *A. fumigatus*. For this purpose, we developed a method to purify conidia-containing phagolysosomes and analyzed their proteomes. By bioinformatical analyses of differentially regulated phagolysosomal proteins we compiled a regulatory module that represents the regulated proteins. By combining the different methods, we deduced a model in which wt conidia modulate endosomal trafficking and fusion processes, intracellular signaling and metabolic pathways to prevent acidification of the phagolysosome, delivery of degradative enzymes, induction of autophagy, apoptosis and pro-inflammatory immune response to survive within the phagolysosome.

Our analysis required the isolation of conidia-containing phagolysosomes. A common protocol to isolate phagolysosomes makes use of the sedimentation properties of the ingested latex beads and was first described by Wetzel *et al*. (39). However, due to the sedimentation properties of conidia-containing phagolysosomes their separation on a sucrose gradient is difficult. Alternatively, Steinhäuser *et al.* described the purification of *Mycobacterium tuberculosis* bacteria-containing phagolysosomes based on magnetic separation (24). The cell lysis was optimized such that the cytoplasmic membrane was disrupted and at the same time the integrity of the phagolysosomal membrane was maintained. A strategy of magnetic separation, protein extraction and concentration was developed to yield the conidia-containing phagolysosomal proteome that could be measured by LC-MS/MS.

The outer phagolysosomal membrane is surrounded by a mesh of sticky actin fibers that trap organelles in its proximity during the isolation procedure (40). The occurrence of proteins typically present in non-phagosomal cell compartments such as the nucleus, ribosomes or mitochondria has been reported earlier (15). Their frequency was especially high in cells with a high autophagocytic activity. This can be

explained by the dynamic interaction and exchange between those two organelles (21, 41). Additionally, mitochondria have been implicated in a broad number of cellular functions, including TLR-dependent ROS production in response to intracellular pathogens (42) and induction of apoptosis *via* intrinsic and extrinsic pathways (43).

The comparison of the protein abundances in the wt and *pksP* mutant conidia-containing phagolysosomes is a challenging endeavor, because of the complexity of the experimental set-up and high variations of the biological replicates. The results of studies on the phagolysosomal proteome vary depending on different factors: (i) the usage of cell lines or primary cells (23), (ii) the ingested particles *e.g.* latex beads, apoptotic cells, pathogen-associated structures or pathogens (16-18, 22), (iii) the age of the phagolysosome (15, 17), (iv) the analyzed fraction *e.g*. entire phagolysosome or membrane domains (detergent-resistant or detergent-soluble membranes) (15) and (v) the activation status of the cells, *i.e.* stimulation with cytokines *prior* to the infection (19).

With the help of a label-free quantification, around 30 % of the identified proteins were classified as significantly regulated. The differential regulation of cathepsin Z, Lamp1 and NADH dehydrogenase was verified by western blotting and the differential recruitment of Vamp8 was confirmed by immunofluorescence. Interestingly, the regulation of mTOR, which was not detected by the LC-MS measurement, but was predicted from the interaction network, was found to be differentially regulated by western blot analysis and thus confirmed the bioinformatics approach. The putative low abundance of mTOR might explain why this protein was only detected by sensitive western blotting but not by LC-MS/MS. The comprehensive LC-MS/MS analysis was based on a bottom-up data-dependent shotgun approach, *i.e.*, not only the general detection sensitivity of the tryptic peptides of a certain protein is decisive. Much more important for highly complex peptide samples is the dynamic range of the analysis. *i.e.*, relative abundance of the tryptic peptides of mTOR in relation to all other peptides, since the 10 most abundant precursor ions per data-dependent scan cycle are selected for fragmentation. Since murine mTOR is a large protein of about 289 kDa, which implicates numerous potentially detectable peptides, it can be assumed that mTOR is of relative low abundance. At least the abundance of mTOR is lower than for all proteins identified in our study.

Taken together, the bioinformatics compilation of the differentially abundant proteins into the regulatory module allowed for an identification of processes that are modified in the phagolysosome after ingestion of either wt or *pksP* conidia.

vATPase-dependent acidification

Acidification of the phagolysosome is prerequisite for the degradation of phagocytosed material and is driven by the vATPase, the vacuolar ATP-dependent proton pump (44). Activity of the enzyme complex is regulated *via* assembly and disassembly of the membrane bound V_0 and cytosolic V_1 domain (45). In a previous study, we showed that activity of the vATPase mainly drives the acidification of phagolysosomes containing *pksP* conidia (14). Here, the proteomic data confirmed the increased abundance of V_1 subunits in *pksP* conidia-containing phagolysosomes.

Lysosome-endosomal trafficking

The endocytic trafficking and transport system is also modulated in the wt conidia-containing phagolysosome. We detected several proteins of the SNARE, SNAP and syntaxin family, which mediate intracellular trafficking, docking and fusion processes (46). They were mainly down-regulated in macrophages infected with wt conidia. Also, the small GTPase Rab5 and early endosomal antigen 1 (EEA1) were regulated. Rab5 and its effector EEA1 mediate homotypic fusion of the early phagosome with early endosomes and are regarded as markers for an early stage of phagolysosomal maturation (47, 48). Rab5 had a lower abundance in wt conidia-containing phagolysosomes, whereas EEA1 was more abundant. Likewise, EH domain-containing proteins, which control endocytic fusion and co-localize with Rab5 and EEA1 were less abundant in wt conidia-containing phagolysosomes. This implies that wt conidia-containing phagosomes are less fusogenic and arrest the maturation of the phagolysosome at an early stage. This finding is in line with earlier observations when we determined the fusion of *A. fumigatus* conidia-containing phagosomes with lysosomes by measuring the localization of the phagolysosomal markers cathepsin D and Lamp1 (13). The reduced acquisitions of those markers by wt conidia-containing phagosomes prompted us to speculate that *A. fumigatus* wt conidia interfere with the endocytic pathway by preventing fusions of the phagosome with lysosomes. However, when we analyzed the fusion rate of dextran beads-containing lysosomes with phagosomes (14), only a slight delay in the delivery of the beads to wt conidia-containing phagosomes was observed. Thus, it is conceivable that *A. fumigatus* conidia do not generally block endocytic fusions, but rather selectively interfere with the delivery of proteins and enzymes required for the maturation of the phagolysosome into a biocidal compartment. An interference with endosomal trafficking and fusions by targeting small Rab GTPases has been reported for many pathogens such as *Candida albicans, Mycobacterium tuberculosis, Coxiella burnetii, Helicobacter pylori, Salmonella enterica, Chlamydia* species and others (reviewed in (49)).

Generation of energy

Components of the oxidative phosphorylation (OXPHOS) system, *i.e.,* protein complexes of the mitochondrial electron transport chain, are enriched in the *pksP* conidia-containing phagolysosomal sample. The occurrence of those components, although they are of non-phagolysosomal origin, might represent a specific effect of mitochondrial involvement in phagolysosomal processes. We found subunits of all four complexes of the electron transport chain as well as 3-ketoacyl-CoA thiolase and acyl-CoA dehydrogenase of the fatty acid β-oxidation enriched in the *pksP* mutant conidia-containing phagolysosome, indicating that wt conidia influence the host cell energy metabolism. In line with this assumption, we found mTOR, a regulator of cellular metabolism (50), enriched in phagolysosomes of macrophages that were challenged with *pksP* conidia. Furthermore, mitochondrial ROS, which are generated by the electron transport chain, were described to contribute to the killing of intracellular pathogens (42, 51).

Intracellular signaling

The proteomic data indicate a reduced presence of components of the Akt-mTOR pathway in the wt conidia-containing phagolysosomal proteome. This signaling axis plays a major role in inducing autophagy under starvation conditions to recycle nutrients from the phagosome. By targeting the autophagy-activating pathways ingested wt conidia interfere with the generation of the biocidal autophagosome (52). In line with this hypothesis, we found components of the autophagy machinery such as Vamp8, Snap29 and Vti1b of the autophagosomal SNARE complex (53) and Rubicon (Run domain Beclin-1-interacting and cysteine-rich domain-containing protein) (54) in the regulated modules confirming a role of this specific intracellular degradation process in the clearance of *A. fumigatus* conidia. Rubicon has recently been identified as the central switch from autophagy to Microtubule-Associated Protein 1 Light Chain 3 (LC3)-associated phagocytosis (LAP), an Atg5-dependent autophagy mechanism, where the LC3BI protein binds phosphatidylethanolamine (PE) to form the active, lipidated LC3BII protein that binds to phagolysosomes (55, 56). Rubicon recruits the NADPH oxidase (NOX) and activates its ROS producing activity, which in turn is required for LC3B lipidation (54). In line, Chamilos *et al.* (52, 57) demonstrated that DHN melanin of *A. fumigatus* conidia blocks LAP activation in macrophages.

Previous work of our lab showed that wt conidia of *A. fumigatus* block apoptosis of macrophages by hijacking the PI3K/Akt signaling pathway (58). The sustained activation of Akt promotes cell survival and inhibits induction of the apoptosis process and likely depicts a strategy of the pathogen to hide inside the macrophage and evade further immune responses (58, 59). Among the differential abundant

proteins were elements of the apoptosis or cell survival regulation pathways: MAPK, AKT, mTOR and Rac signaling pathway, the ubiquitin-proteasome system, members of the 14-3-3 family proteins, prostaglandin E synthase among others. Pro-apoptotic proteins such as Bak1 (60), Aifm2 and Praf2 were higher abundant in *pksP* mutant conidia-containing phagolysosomes, whereas the anti-apoptotic regulator Bcl2-like 13 protein was enriched in wt conidia-containing phagolysosomes.

Degradation and antigen processing capacity

Different studies demonstrated the requirement for ROS for an efficient fungal clearance (61, 62). ROS are generated by the NOX complex which consists of five subunits. Our data suggest impaired NOX assembly and, thus, reduced production of ROS after ingestion of wt conidia, because one of the five NOX subunits, $p47^{phox}$ (Ncf1) was less abundant in wt conidia-containing phagolysosomes. Also, up-stream elements of the Rac GTP-binding protein family, which regulate NOX assembly, such as guanine nucleotide exchange factors (GEFs) ArhGEFs and Rac GTPase activating protein (RacGAP1) showed low levels in the wt sample. Langfelder *et al.* showed a ten-fold increase in ROS production of PMNs that were challenged with *A. fumigatus pksP* mutant conidia compared to wt conidia (12). Jahn *et al.* demonstrated that this increase can be attributed at least in part to the fact that *pksP* mutant conidia lack ROS quenching by DHN melanin (63). Besides its fungicidal activity, signaling function was also ascribed to ROS in mediating the induction of the autophagy machinery (64) and pro-apoptotic signaling (58, 65). Consistently, Volling *et al.* hypothesized that DHN melanin inhibits apoptosis by quenching ROS (58, 63).

Cathepsins, lysosomal peptidases and enzymes to degrade glycans and glycolipids were enriched in the proteome of *pksP* mutant conidia-containing phagolysosomes indicating a reduced degradation capacity of wt conidia-containing phagolysosomes. In line with this finding is the reduced antigen processing and presentation machinery of those phagolysosomes. For example, phagolysosomes containing wt conidia had lower levels of the macrophage activation marker CD68 or macrophage colony-stimulating factor receptor 1 (CSFR1).

The interference of *A. fumigatus* with the described intracellular processes of macrophages is conceivably due to an interaction of fungal proteins with host proteins. We performed an initial bioinformatics analysis to predict potential interaction candidates on the basis of already described host-pathogen protein interactions. This analysis suggests fungal heat shock proteins Hsp70 and 90, the translation elongation factor Tef1 and a 14-3-3 protein ArtA to interact with a range of host proteins

involved in processes such as vATPase activity, endocytic trafficking and signaling (Fig. S1). Experiments evaluating the prediction of these interactions, *e.g*. on a biochemical level or using immune cells with a knock down of the genes of interest, are required to identify the role of protein-protein interactions for the immune modulation by *A. fumigatus.*

Altogether, this study provides a detailed map of proteins and a comprehensive overview of macrophage intracellular processes that are regulated upon ingestion of *A. fumigatus* conidia. It delivers a protocol to obtain conidia-containing phagolysosomes, a bioinformatics method for integrating quantitative LC-MS/MS data into the context of the entire protein-protein interaction network to identify significantly regulated processes and confirms previous findings about the *A. fumigatus* immune evasion strategy, *i.e.*, inhibition of vATPase-dependent phagolysosomal acidification and the prevention of apoptosis induction. Intriguingly, our data suggest an interference of wt conidia with endocytic vesicle trafficking, MAPK and mTOR signaling, ROS production *via* NADPH oxidase, and degradative functions of the phagolysosome. Further, the reprogramming of energy metabolism and activation of macrophage immune responses, has not been reported before. These findings lay the basis for mechanistic studies that will help to unravel the complexity of immune evasion strategies of *A. fumigatus*.

REFERENCES

1. Brown, G. D., Denning, D. W., Gow, N. A., Levitz, S. M., Netea, M. G., and White, T. C. (2012) Hidden killers: human fungal infections. *Sci Transl Med* 4, 165rv113
2. Kontoyiannis, D. P., Marr, K. A., Park, B. J., Alexander, B. D., Anaissie, E. J., Walsh, T. J., Ito, J., Andes, D. R., Baddley, J. W., Brown, J. M., Brumble, L. M., Freifeld, A. G., Hadley, S., Herwaldt, L. A., Kauffman, C. A., Knapp, K., Lyon, G. M., Morrison, V. A., Papanicolaou, G., Patterson, T. F., Perl, T. M., Schuster, M. G., Walker, R., Wannemuehler, K. A., Wingard, J. R., Chiller, T. M., and Pappas, P. G. (2010) Prospective surveillance for invasive fungal infections in hematopoietic stem cell transplant recipients, 2001-2006: overview of the Transplant-Associated Infection Surveillance Network (TRANSNET) Database. *Clin Infect Dis* 50, 1091-1100
3. Heinekamp, T., Schmidt, H., Lapp, K., Pahtz, V., Shopova, I., Koster-Eiserfunke, N., Kruger, T., Kniemeyer, O., and Brakhage, A. A. (2015) Interference of *Aspergillus fumigatus* with the immune response. *Semin Immunopathol* 37, 141-152
4. Dagenais, T. R., and Keller, N. P. (2009) Pathogenesis of *Aspergillus fumigatus* in invasive aspergillosis. *Clin Microbiol Rev* 22, 447-465
5. Park, S. J., and Mehrad, B. (2009) Innate immunity to *Aspergillus* species. *Clin Microbiol Rev* 22, 535-551
6. Thi, E. P., Lambertz, U., and Reiner, N. E. (2012) Sleeping with the enemy: how intracellular pathogens cope with a macrophage lifestyle. *PLoS Pathog* 8, e1002551
7. Koul, A., Herget, T., Klebl, B., and Ullrich, A. (2004) Interplay between *Mycobacteria* and host signalling pathways. *Nat Rev Microbiol* 2, 189-202

8. Meresse, S., Steele-Mortimer, O., Moreno, E., Desjardins, M., Finlay, B., and Gorvel, J. P. (1999) Controlling the maturation of pathogen-containing vacuoles: a matter of life and death. *Nat Cell Biol* 1, E183-188
9. Heinekamp, T., Thywissen, A., Macheleidt, J., Keller, S., Valiante, V., and Brakhage, A. A. (2012) *Aspergillus fumigatus* melanins: interference with the host endocytosis pathway and impact on virulence. *Front Microbiol* 3, 440
10. Slesiona, S., Gressler, M., Mihlan, M., Zaehle, C., Schaller, M., Barz, D., Hube, B., Jacobsen, I. D., and Brock, M. (2012) Persistence versus escape: *Aspergillus terreus* and *Aspergillus fumigatus* employ different strategies during interactions with macrophages. *PLoS One* 7, e31223
11. Jahn, B., Koch, A., Schmidt, A., Wanner, G., Gehringer, H., Bhakdi, S., and Brakhage, A. A. (1997) Isolation and characterization of a pigmentless-conidium mutant of *Aspergillus fumigatus* with altered conidial surface and reduced virulence. *Infect Immun* 65, 5110-5117
12. Langfelder, K., Jahn, B., Gehringer, H., Schmidt, A., Wanner, G., and Brakhage, A. A. (1998) Identification of a polyketide synthase gene (*pksP*) of *Aspergillus fumigatus* involved in conidial pigment biosynthesis and virulence. *Med Microbiol Immunol* 187, 79-89
13. Jahn, B., Langfelder, K., Schneider, U., Schindel, C., and Brakhage, A. A. (2002) PKSP-dependent reduction of phagolysosome fusion and intracellular kill of *Aspergillus fumigatus* conidia by human monocyte-derived macrophages. *Cell Microbiol* 4, 793-803
14. Thywissen, A., Heinekamp, T., Dahse, H. M., Schmaler-Ripcke, J., Nietzsche, S., Zipfel, P. F., and Brakhage, A. A. (2011) Conidial dihydroxynaphthalene melanin of the human pathogenic fungus *Aspergillus fumigatus* interferes with the host endocytosis pathway. *Front Microbiol* 2, 96
15. Goyette, G., Boulais, J., Carruthers, N. J., Landry, C. R., Jutras, I., Duclos, S., Dermine, J. F., Michnick, S. W., LaBoissiere, S., Lajoie, G., Barreiro, L., Thibault, P., and Desjardins, M. (2012) Proteomic characterization of phagosomal membrane microdomains during phagolysosome biogenesis and evolution. *Mol Cell Proteomics* 11, 1365-1377
16. Rogers, L. D., and Foster, L. J. (2007) The dynamic phagosomal proteome and the contribution of the endoplasmic reticulum. *Proc Natl Acad Sci U S A* 104, 18520-18525
17. Dill, B. D., Gierlinski, M., Hartlova, A., Arandilla, A. G., Guo, M., Clarke, R. G., and Trost, M. (2015) Quantitative proteome analysis of temporally resolved phagosomes following uptake *via* key phagocytic receptors. *Mol Cell Proteomics* 14, 1334-1349
18. Lee, B. Y., Jethwaney, D., Schilling, B., Clemens, D. L., Gibson, B. W., and Horwitz, M. A. (2010) The *Mycobacterium bovis* bacille Calmette-Guerin phagosome proteome. *Mol Cell Proteomics* 9, 32-53
19. Trost, M., English, L., Lemieux, S., Courcelles, M., Desjardins, M., and Thibault, P. (2009) The phagosomal proteome in interferon-γ-activated macrophages. *Immunity* 30, 143-154
20. Shui, W., Gilmore, S. A., Sheu, L., Liu, J., Keasling, J. D., and Bertozzi, C. R. (2009) Quantitative proteomic profiling of host-pathogen interactions: the macrophage response to Mycobacterium tuberculosis lipids. *J Proteome Res* 8, 282-289
21. Shui, W., Sheu, L., Liu, J., Smart, B., Petzold, C. J., Hsieh, T. Y., Pitcher, A., Keasling, J. D., and Bertozzi, C. R. (2008) Membrane proteomics of phagosomes suggests a connection to autophagy. *Proc Natl Acad Sci U S A* 105, 16952-16957
22. Shui, W., Petzold, C. J., Redding, A., Liu, J., Pitcher, A., Sheu, L., Hsieh, T., Keasling, J. D., and Bertozzi, C. R. (2011) Organelle membrane proteomics reveals differential influence of mycobacterial lipoglycans on macrophage phagosome maturation and autophagosome accumulation. *J Proteome Res* 339, 339-348
23. Guo, M., Hartlova, A., Dill, B. D., Prescott, A. R., Gierlinski, M., and Trost, M. (2015) High-resolution quantitative proteome analysis reveals substantial differences between phagosomes of RAW 264.7 and bone marrow derived macrophages. *Proteomics* 15, 3169-3174

24. Steinhauser, C., Heigl, U., Tchikov, V., Schwarz, J., Gutsmann, T., Seeger, K., Brandenburg, J., Fritsch, J., Schroeder, J., Wiesmuller, K. H., Rosenkrands, I., Walther, P., Pott, J., Krause, E., Ehlers, S., Schneider-Brachert, W., Schutze, S., and Reiling, N. (2013) Lipid-labeling facilitates a novel magnetic isolation procedure to characterize pathogen-containing phagosomes. *Traffic* 14, 321-336
25. Wessel, D., and Flugge, U. I. (1984) A method for the quantitative recovery of protein in dilute solution in the presence of detergents and lipids. *Anal Biochem* 138, 141-143
26. Faden, F., Eschen-Lippold, L., and Dissmeyer, N. (2016) Normalized Quantitative Western Blotting Based on Standardized Fluorescent Labeling. *Methods Mol Biol* 1450, 247-258
27. Silva, J. C., Gorenstein, M. V., Li, G. Z., Vissers, J. P., and Geromanos, S. J. (2006) Absolute quantification of proteins by LCMSE: a virtue of parallel MS acquisition. *Mol Cell Proteomics* 5, 144-156
28. Vizcaino, J. A., Csordas, A., del-Toro, N., Dianes, J. A., Griss, J., Lavidas, I., Mayer, G., Perez-Riverol, Y., Reisinger, F., Ternent, T., Xu, Q. W., Wang, R., and Hermjakob, H. (2016) 2016 update of the PRIDE database and its related tools. *Nucleic Acids Res* 44, D447-456
29. Vlaic, S., Conrad, T., Tokarski-Schnelle, C., Gustafsson, M., Dahmen, U., Guthke, R., and Schuster, S. (2018) ModuleDiscoverer: Identification of regulatory modules in protein-protein interaction networks. *Sci Rep* 8, 433
30. Barrenas, F., Chavali, S., Alves, A. C., Coin, L., Jarvelin, M. R., Jornsten, R., Langston, M. A., Ramasamy, A., Rogers, G., Wang, H., and Benson, M. (2012) Highly interconnected genes in disease-specific networks are enriched for disease-associated polymorphisms. *Genome Biol* 13, R46
31. Falcon, S., and Gentleman, R. (2007) Using GOstats to test gene lists for GO term association. *Bioinformatics* 23, 257-258
32. Carlson, M. org.Mm.eg.db: Genome wide annotation for Mouse. R package version 3.2.3., https://bioconductor.org/
33. Kinsella, R. J., Kahari, A., Haider, S., Zamora, J., Proctor, G., Spudich, G., Almeida-King, J., Staines, D., Derwent, P., Kerhornou, A., Kersey, P., and Flicek, P. (2011) Ensembl BioMarts: a hub for data retrieval across taxonomic space. *Database* Vol. 2011, Article ID bar030
34. Durinck, S., Spellman, P. T., Birney, E., and Huber, W. (2009) Mapping identifiers for the integration of genomic datasets with the R/Bioconductor package biomaRt. *Nat Protoc* 4, 1184-1191
35. Remmele, C. W., Luther, C. H., Balkenhol, J., Dandekar, T., Muller, T., and Dittrich, M. T. (2015) Integrated inference and evaluation of host-fungi interaction networks. *Front Microbiol* 6, 764
36. Desjardins, M., Huber, L. A., Parton, R. G., and Griffiths, G. (1994) Biogenesis of phagolysosomes proceeds through a sequential series of interactions with the endocytic apparatus. *J Cell Biol* 124, 677-688
37. Szklarczyk, D., Franceschini, A., Wyder, S., Forslund, K., Heller, D., Huerta-Cepas, J., Simonovic, M., Roth, A., Santos, A., Tsafou, K. P., Kuhn, M., Bork, P., Jensen, L. J., and von Mering, C. (2015) STRING v10: protein-protein interaction networks, integrated over the tree of life. *Nucleic Acids Res* 43, D447-452
38. Asif, A. R., Oellerich, M., Amstrong, V. W., Riemenschneider, B., Monod, M., and Reichard, U. (2006) Proteome of conidial surface associated proteins of Aspergillus fumigatus reflecting potential vaccine candidates and allergens. *J Proteome Res* 5, 954-962
39. Wetzel, M. G., and Korn, E. D. (1969) Phagocytosis of latex beads by Acahamoeba castellanii (Neff). 3. Isolation of the phagocytic vesicles and their membranes. *J Cell Biol* 43, 90-104
40. Garin, J., Diez, R., Kieffer, S., Dermine, J. F., Duclos, S., Gagnon, E., Sadoul, R., Rondeau, C., and Desjardins, M. (2001) The phagosome proteome: insight into phagosome functions. *J Cell Biol* 152, 165-180
41. Sanjuan, M. A., Dillon, C. P., Tait, S. W., Moshiach, S., Dorsey, F., Connell, S., Komatsu, M., Tanaka, K., Cleveland, J. L., Withoff, S., and Green, D. R. (2007) Toll-like receptor signalling in macrophages links the autophagy pathway to phagocytosis. *Nature* 450, 1253-1257

42. West, A. P., Brodsky, I. E., Rahner, C., Woo, D. K., Erdjument-Bromage, H., Tempst, P., Walsh, M. C., Choi, Y., Shadel, G. S., and Ghosh, S. (2011) TLR signalling augments macrophage bactericidal activity through mitochondrial ROS. *Nature* 472, 476-480
43. Wang, C., and Youle, R. J. (2009) The role of mitochondria in apoptosis. *Annu Rev Genet* 43, 95-118
44. Haas, A. (2007) The phagosome: compartment with a license to kill. *Traffic* 8, 311-330
45. Lafourcade, C., Sobo, K., Kieffer-Jaquinod, S., Garin, J., and van der Goot, F. G. (2008) Regulation of the V-ATPase along the endocytic pathway occurs through reversible subunit association and membrane localization. *PLoS One* 3, e2758
46. Waters, M. G., and Hughson, F. M. (2000) Membrane tethering and fusion in the secretory and endocytic pathways. *Traffic* 1, 588-597
47. Christoforidis, S., McBride, H. M., Burgoyne, R. D., and Zerial, M. (1999) The Rab5 effector EEA1 is a core component of endosome docking. *Nature* 397, 621-625
48. Simonsen, A., Lippe, R., Christoforidis, S., Gaullier, J. M., Brech, A., Callaghan, J., Toh, B. H., Murphy, C., Zerial, M., and Stenmark, H. (1998) EEA1 links PI(3)K function to Rab5 regulation of endosome fusion. *Nature* 394, 494-498
49. Brumell, J. H., and Scidmore, M. A. (2007) Manipulation of Rab GTPase function by intracellular bacterial pathogens. *Microbiol Mol Biol Rev* 71, 636-652
50. Byles, V., Covarrubias, A. J., Ben-Sahra, I., Lamming, D. W., Sabatini, D. M., Manning, B. D., and Horng, T. (2013) The TSC-mTOR pathway regulates macrophage polarization. *Nat Commun* 4, 2834
51. Roca, F. J., and Ramakrishnan, L. (2013) TNF dually mediates resistance and susceptibility to mycobacteria via mitochondrial reactive oxygen species. *Cell* 153, 521-534
52. Chamilos, G., Akoumianaki, T., Kyrmizi, I., Brakhage, A. A., Beauvais, A., and Latge, J. P. (2016) Melanin targets LC3-associated phagocytosis (LAP): a novel pathogenetic mechanism in fungal disease. *Autophagy* 12, 888-889
53. Diao, J., Liu, R., Rong, Y., Zhao, M., Zhang, J., Lai, Y., Zhou, Q., Wilz, L. M., Li, J., Vivona, S., Pfuetzner, R. A., Brunger, A. T., and Zhong, Q. (2015) ATG14 promotes membrane tethering and fusion of autophagosomes to endolysosomes. *Nature* 520, 563-566
54. Zhong, Y., Wang, Q. J., Li, X., Yan, Y., Backer, J. M., Chait, B. T., Heintz, N., and Yue, Z. (2009) Distinct regulation of autophagic activity by Atg14L and Rubicon associated with Beclin 1-phosphatidylinositol-3-kinase complex. *Nat Cell Biol* 11, 468-476
55. Boyle, K. B., and Randow, F. (2015) Rubicon swaps autophagy for LAP. *Nat Cell Biol* 17, 843-845
56. Martinez, J., Malireddi, R. K., Lu, Q., Dias Cunha, L., Pelletier, S., Gingras, S., Orchard, R., Guan, J. L., Tan, H., Peng, J., Kanneganti, T. D., Virgin, H. W., and Green, D. R. (2015) Molecular characterization of LC3-associated phagocytosis reveals distinct roles for Rubicon, NOX2 and autophagy proteins. *Nat Cell Biol* 17, 893-906
57. Akoumianaki, T., Kyrmizi, I., Valsecchi, I., Gresnigt, M. S., Samonis, G., Drakos, E., Boumpas, D., Muszkieta, L., Prevost, M. C., Kontoyiannis, D. P., Chavakis, T., Netea, M. G., van de Veerdonk, F. L., Brakhage, A. A., El-Benna, J., Beauvais, A., Latge, J. P., and Chamilos, G. (2016) *Aspergillus* cell wall melanin blocks LC3-associated phagocytosis to promote pathogenicity. *Cell Host Microbe* 19, 79-90
58. Volling, K., Thywissen, A., Brakhage, A. A., and Saluz, H. P. (2011) Phagocytosis of melanized *Aspergillus* conidia by macrophages exerts cytoprotective effects by sustained PI3K/Akt signalling. *Cell Microbiol* 13, 1130-1148
59. Volling, K., Brakhage, A. A., and Saluz, H. P. (2007) Apoptosis inhibition of alveolar macrophages upon interaction with conidia of *Aspergillus fumigatus*. *FEMS Microbiol Lett* 275, 250-254
60. Pardo, J., Urban, C., Galvez, E. M., Ekert, P. G., Muller, U., Kwon-Chung, J., Lobigs, M., Mullbacher, A., Wallich, R., Borner, C., and Simon, M. M. (2006) The mitochondrial protein Bak is pivotal

for gliotoxin-induced apoptosis and a critical host factor of *Aspergillus fumigatus* virulence in mice. *J Cell Biol* 174, 509-519
61. Philippe, B., Ibrahim-Granet, O., Prevost, M. C., Gougerot-Pocidalo, M. A., Sanchez Perez, M., Van der Meeren, A., and Latge, J. P. (2003) Killing of *Aspergillus fumigatus* by alveolar macrophages is mediated by reactive oxidant intermediates. *Infect Immun* 71, 3034-3042
62. Grimm, M. J., Vethanayagam, R. R., Almyroudis, N. G., Dennis, C. G., Khan, A. N., D'Auria, A. C., Singel, K. L., Davidson, B. A., Knight, P. R., Blackwell, T. S., Hohl, T. M., Mansour, M. K., Vyas, J. M., Rohm, M., Urban, C. F., Kelkka, T., Holmdahl, R., and Segal, B. H. (2013) Monocyte- and macrophage-targeted NADPH oxidase mediates antifungal host defense and regulation of acute inflammation in mice. *J Immunol* 190, 4175-4184
63. Jahn, B., Boukhallouk, F., Lotz, J., Langfelder, K., Wanner, G., and Brakhage, A. A. (2000) Interaction of human phagocytes with pigmentless *Aspergillus* conidia. *Infect Immun* 68, 3736-3739
64. Huang, J., Canadien, V., Lam, G. Y., Steinberg, B. E., Dinauer, M. C., Magalhaes, M. A., Glogauer, M., Grinstein, S., and Brumell, J. H. (2009) Activation of antibacterial autophagy by NADPH oxidases. *Proc Natl Acad Sci U S A* 106, 6226-6231
65. Jacobson, M. D. (1996) Reactive oxygen species and programmed cell death. *Trends Biochem Sci* 21, 83-86

Footnotes

Funding Sources: This work was supported by the excellence graduate school Jena School for Microbial Communication JSMC and the CRC/Transregio 124 Human-pathogenic fungi and their human host - Networks of interaction - FungiNet, funded by the Deutsche Forschungsgemeinschaft (projects A1, B2 and Z2) as well as the InfectControl-project FINAR funded by the German Ministry for Education and Research (BMBF) and the Leibniz Science Campus InfectoOptics (project HotAim). Andreas Thywissen is gratefully acknowledged for initial experiments and Silke Steinbach for excellent technical assistance.

Data Availability

Data sets are available at the PRIDE database under the Project ID: PXD006134 URL: https://www.ebi.ac.uk/pride/archive/projects/PXD006134

Figures

Figure 1: Flowchart for the purification of conidia-containing phagolysosomes, proteome detection and data analysis. The procedure starts with magnetic labeling of conidia that are then incubated with macrophages for 2 h. The cell lysate is loaded onto a magnetic column to separate the magnetic fraction

from the cell debris. The protein is extracted on-column, then precipitated and concentrated for LC-MS/MS measurement. After label-free quantification the data was analyzed to identify regulated proteins and modules.

Figure 2: Effect of magnetic labeling on characteristics of conidia. Magnetic labeling of conidia has no effect on phagocytosis and acidification of phagolysosomes (PLs). **A)** The phagocytosis ratio was determined after 2 h co-incubation of macrophages with magnetically labeled or unlabeled conidia of the wt and the *pksP* mutant. **B)** The ratio of acidified phagolysosomes was determined 2 h post-infection of macrophages with conidia. **C)** Integrity of the phagolysosomal membrane is not impaired by isolation of conidia-containing phagolysosomes. Cells were loaded overnight with fluorescent dextran beads. Conidia were labeled with CFW and added to the cells for 2 h. Cell lysis was performed by shearing the cell suspension and the lysate stained with DiD, specific for eukaryotic cell membranes. Images show a triple staining of particles with dextran, DiD and CFW indicating an intact phagolysosomal compartment.

Figure 3: Host regulatory module. A total of 302 proteins are connected by 3448 edges in the displayed module. 178 proteins were detected in the LC-MS/MS analysis and 109 classified as differentially regulated. The graph displays regions of the protein-protein interactome that are significantly enriched and shown here to be differently regulated. The color scale from *blue* to *yellow* represents the $\log_2$ fold change of protein abundances, proteins in *grey* were not detected by mass spectrometry, but complete the respective submodule due to their close connectivity to the neighboring partner. The *edge size* is indicative of the confidence score of the interaction.

Figure 4: Recruitment of proteins to the phagolysosomal membrane. A) The effect of magnetic labeling on recruitment of cathepsin D to the phagolysosomal membrane 2 h post infection was determined by immunofluorescence. Columns represent mean values of the proportion of cathepsin D-positive phagolysosomes (PLs) +/- SDs. **B)** Western blot analyses were performed to determine abundances of selected proteins in the phagolysosomal fraction. 16 or 8 µg of protein extract from purified wt or *pksP* mutant conidia-containing phagolysosomes were separated by SDS-PAGE. Antibodies against selected candidate proteins from the proteome data were applied. Due to the lack of suitable house-keeping proteins the samples were mixed with the Smart Protein Layer kit that enabled a normalization of the bands to the total loaded protein. **C)** wt conidia-containing phagolysosomes fail to recruit Vamp8. Images are representative of Vamp8 immunofluorescence staining of macrophages 2 h post infection with wt or *pksP* mutant conidia at an MOI = 2. Scale bars refer to 10 µm and arrows indicate Vamp8-

positive phagolysosomes. Columns represent the mean values of the proportion of Vamp8-positive phagolysosomes +/- SDs.

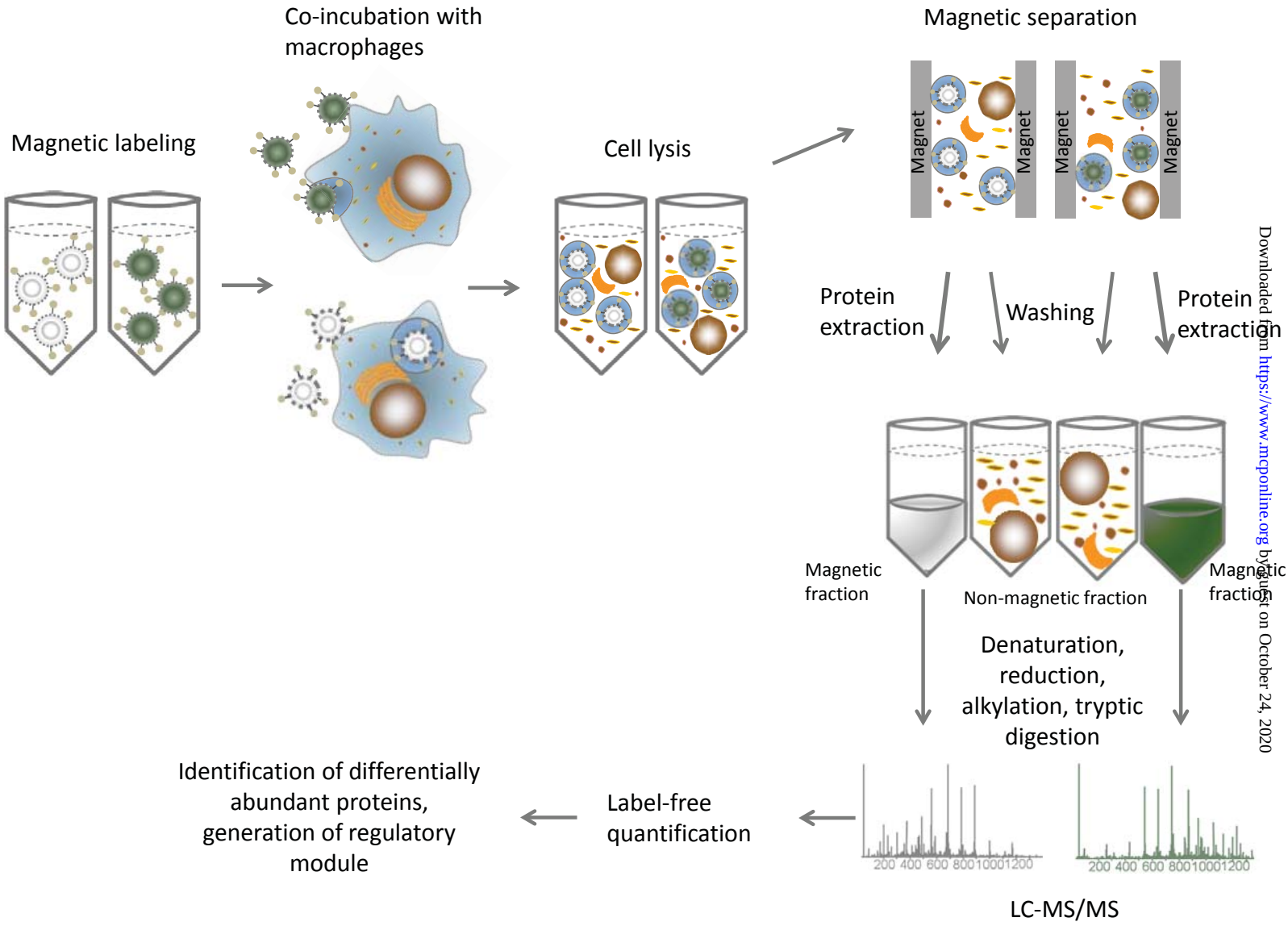

Figure 1

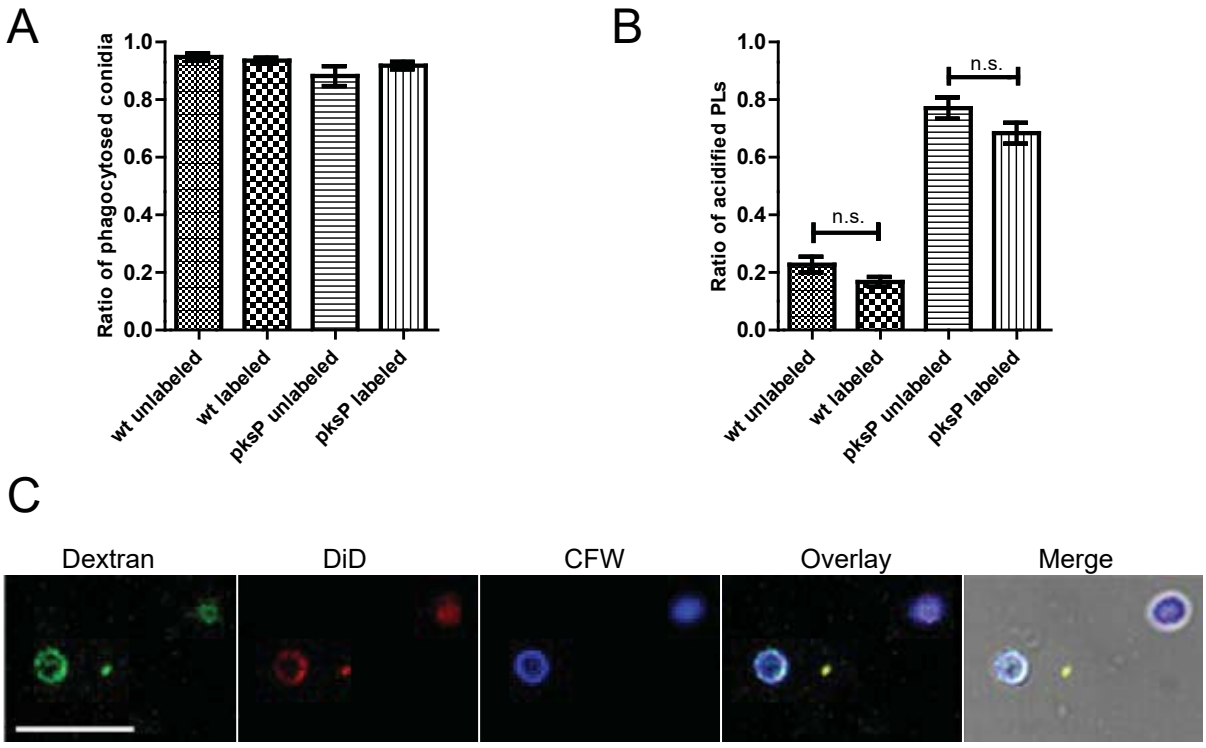

Figure 2

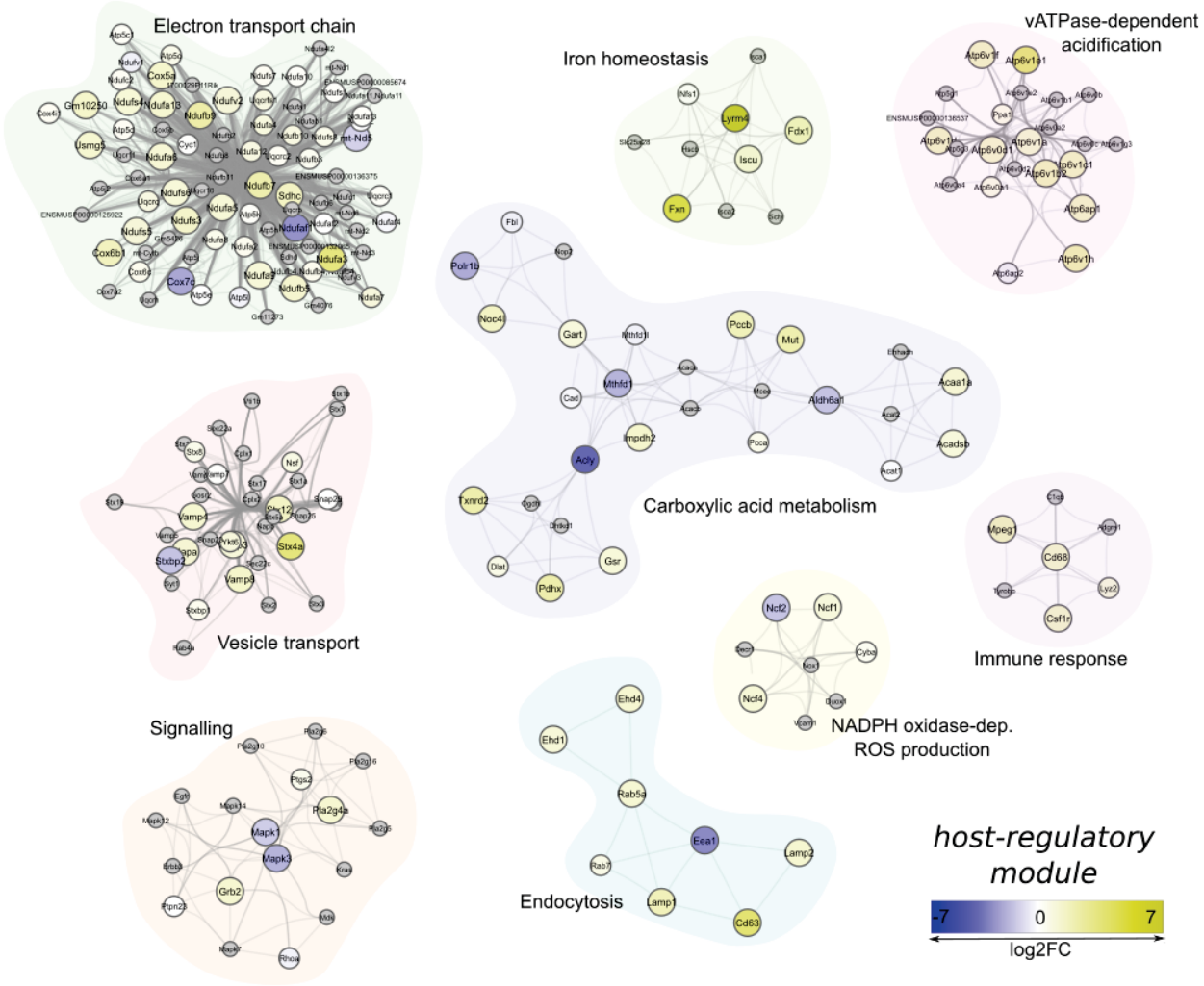

Figure 3

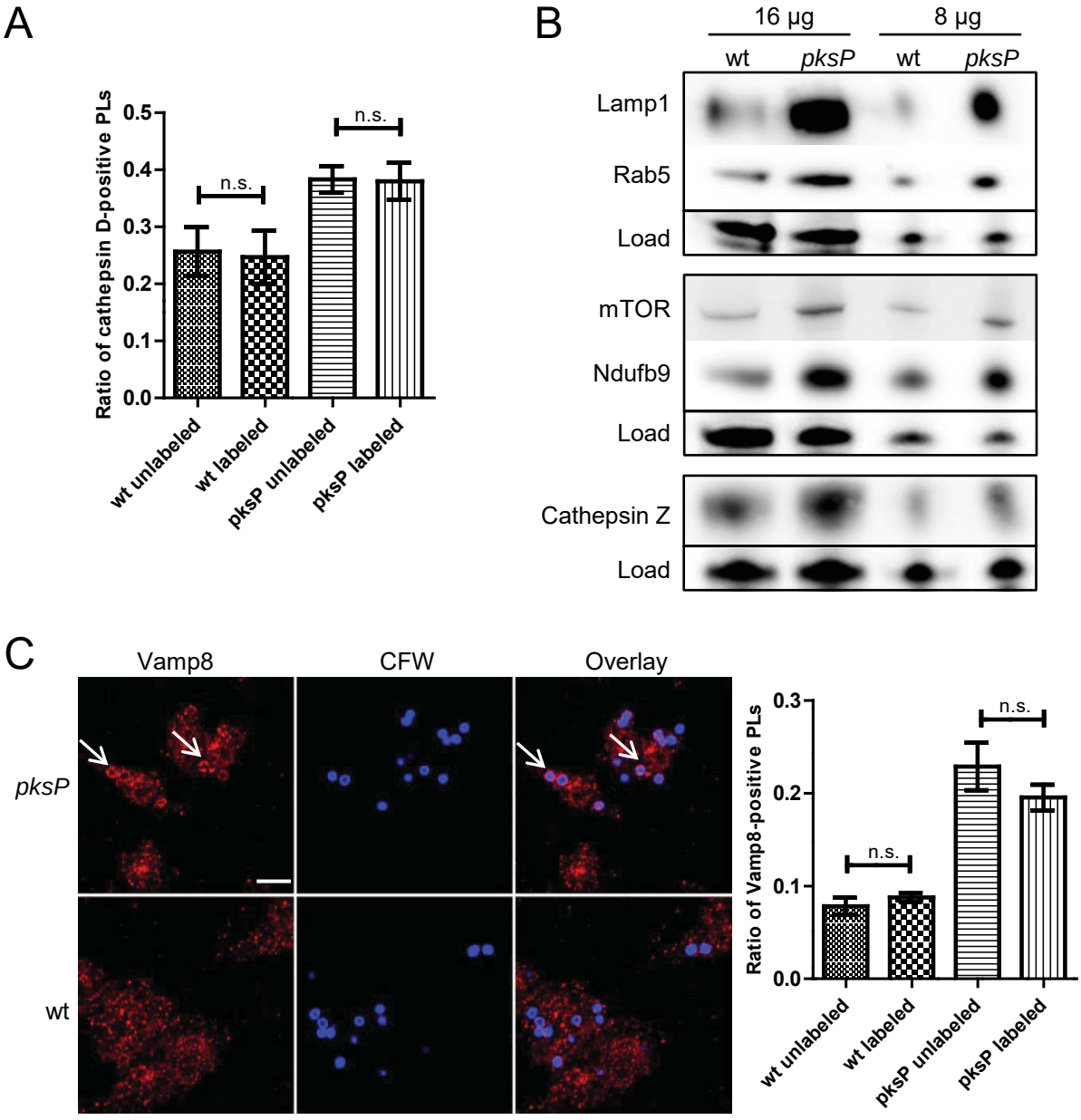

Figure 4